Eur. Phys. J. B **4**, 307–312 (1998)

THE EUROPEAN PHYSICAL JOURNAL B

Polyelectrolyte/post collisions during electrophoresis: Influence of hydrodynamic interactions

P. André[a], D. Long, and A. Ajdari

Laboratoire de Physico-Chimie Théorique, ESA CNRS 7083, ESPCI, 10 rue Vauquelin, 75231 Paris Cedex 05, France

Received: 18 March 1998 / Received in final form and accepted: 20 May 1998

Abstract. We consider the interaction of an homogeneous polyelectrolyte with an obstacle during electrophoretic drift. We explicitly take into account the hydrodynamic interactions generated by this mechanical trapping, and we evaluate their influence on the unhooking process. Important qualitative effects are pointed out in low and moderate field regimes. However, numerical simulations indicate that, in strong field, the existing simpler local force models, which neglect these hydrodynamic interactions, are quantitatively acceptable.

PACS. 87.15.He Molecular dynamics and conformational changes – 82.45.+z Electrochemistry and electrophoresis – 36.20.-r Macromolecules and polymer molecules

1 Introduction

1.1 Aim

The separation of charged macromolecules according to their size is both a technical and a scientific issue. Genetic engineering extensively relies on the fractionation of DNA, a semi-flexible polyelectrolyte, for which electrophoresis, *i.e.* electric field driven migration, is the most widespread technique. The mobility of polyelectrolytes in free solution being size independent, electrophoresis is often performed in gels, which act as sieving media, under constant or pulsed field (to prevent permanent chain alignment that leads to uniform velocity) [1–3]. However, for very large DNA chains, this technique becomes time consuming, inaccurate and even impossible to perform beyond a certain size. Microlithographically etched arrays of posts have recently been suggested as an alternative sieving medium that would allow obstacle geometry optimization, and sample retrieval [4–6].

In order to improve the microscopic control of the separation in the latter systems, one must analyze the unit process of a chain's migration in such media: the collision of a polyelectrolyte with a fixed obstacle under electric field. In the dilute limit we will consider here, it is legitimate to single out this event, but the process is qualitatively different when the post concentration is such that a chain interacts with many obstacles simultaneously [4,6].

Several authors have addressed this collision problem, and have developed numerical simulations based on the same local friction model [7,8]. The polymer is modeled as a Rouse-like bead-spring polyelectrolyte, where each monomer locally contributes to the friction: no hydrodynamic interactions are taken into account, neither between the polymer and the post, nor within the coil itself. The motivation for this last assumption is that it correctly describes the free flow electrophoretic motion of homogeneous polyelectrolytes, and that it also provides a substantial simplification for numerical calculations.

However, recent theoretical elements lead us to question the applicability of this "local force" picture [9,10]. *Between* collisions, a polyelectrolyte is "free draining": in purely electro-osmotic situation, hydrodynamic interactions are negligible and the coil drifts, transparent to the solvent. But *during* a collision, the obstacle applies on the polymer a non-electric force, which, as we recall below, gives rise to unscreened hydrodynamic interactions (not taken in account into the Rouse-like model). Following the analysis developed in [9], we will evaluate the effects of these interactions qualitatively (Sect. 2), then numerically in the strong field regime (Sect. 3). In both sections, we will compare the results of our model including hydrodynamic interactions with that of the local force Rouse-like model, denoted "HI" and "R" respectively.

1.2 Notations and recent results for an end-anchored chain

Let us first recall the difference between free flow electrophoresis and the case of an end-anchored polyelectrolyte under an electric field $\mathbf{E}$. This example, as discussed in [9], illustrates the role of hydrodynamic interactions, and will be a useful guide line in the following section.

[a] e-mail: andre@hogarth.pct.espci.fr

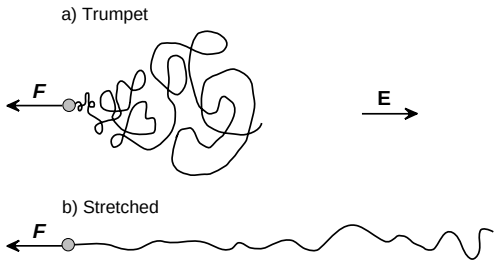

Fig. 1. Schematic configurations of a positively charged chain under: a) intermediate field, b) strong field. The force F from the post maintains the anchored extremity immobile.

In this paper, the polymer is pictured as a uniformly charged Gaussian chain of rigid segments, without excluded volume effects. We use the same frame of assumptions regarding the linearity of electric and non electric effects as in [9]. Notations are the following: the chain's contour length is Na, with a the persistence length, its extension in the direction of the driving field is noted $\mathcal{L}$, and its radius of gyration $R_g \sim aN^\nu$, ν being the Flory exponent. The fluid viscosity is noted η, and the ionic strength is supposed high enough for the Debye-Hückel screening length κ^{-1} to be smaller or of the same order than a. The free drift velocity is $\mathbf{V} = \mu\mathbf{E}$, where μ is the electrophoretic mobility. The Rouse model characterizes the chain by a local charge q and a local friction $\lambda \sim \eta a$, per persistence length.

In free flow electrophoresis, the flow due to counterions exactly cancels the hydrodynamic Stokes flow induced by the motion of the monomers: long range interactions are screened, [11,12]. Thus, μ is independent of size and configuration, and a pure electrophoretic drag does not generate chain deformation. In the Rouse picture, the balance of the extensive electric and viscous forces happens to lead also to a size independent mobility $\mu_R = q/\lambda$, allowing formal identification of the two pictures ($\mu \equiv \mu_R$).

On the other hand, the stretching of an anchored polyelectrolyte is caused by the anchoring force F only, as the electric field alone is unable to deform the chain (Fig. 1). The chain is now immobile, so F alone would pull the anchored point at $\mathbf{V} = -\mu\mathbf{E}$. Therefore the deformation and equilibrium conformation of this polyelectrolyte can be derived from an hydrodynamic equivalent picture: an anchored chain in a solvent flowing at speed $\mu\mathbf{E}$ [9,10]. Consequently F scales like the extension, $F_{HI} = \eta\mu\mathcal{L}E$; whereas with a Rouse-like model, where hydrodynamic interactions are ignored, F would appear proportional to the contour length, $F_R = NqE$.

Three field regimes can be distinguished:

1) *Weak field:* $E < E_c$. The coil is not deformed, $\mathcal{L} \sim N^\nu$. This holds until $F \sim k_BT/R_g$, corresponding to a field deformation threshold $E_{cHI} \sim N^{-2\nu}$, whereas the local force model yields $E_{cR} \sim N^{-(1+\nu)}$.

2) *Intermediate field:* $E_c < E < E^*$. The chain stretches into a trumpet of size $\mathcal{L}_{HI} \sim N^{\frac{\nu}{(2\nu-1)}} E^{\frac{(1-\nu)}{(2\nu-1)}}$ (while $\mathcal{L}_R \sim N^{\frac{1}{\nu}} E^{(\frac{1}{\nu}-1)}$) [13,14]. This extension depends thus on hydrodynamic interactions, and so does the elongation time $t \sim \mathcal{L}/\mu E$. This regime holds until $F \sim k_BT/a$, that is for $E^* \sim k_BT/\eta\mu Na^2$ in both models, when Gaussian elasticity breaks down, due to the finite extensibility of the chain.

3) *Strong field:* $E > E^*$. The chain is almost fully extended, so $\mathcal{L} \sim N$, in both models.

From this example, we clearly see that the combined actions of electric and "neutral" forces give rise to hydrodynamic interactions that are likely to affect scaling laws.

2 Qualitative analysis of the polyelectrolyte/obstacle collision problem

Let us now consider the "collision" of a polyelectrolyte with a post during electrophoresis. Our first point is to determine the trapping threshold field E_c; we then present a qualitative picture of the unhooking process for $E > E_c$, emphasizing the role of hydrodynamic interactions; we conclude this section with a closer look at these interactions in the strong field regime. This last point will bring us to the more quantitative analysis of Section 3.

In this paper, the following simplifications are made: the obstacle is a fixed cylinder, perpendicular to the field. The post is neutral and its radius is supposed small compared to the chain's persistence length, therefore specific chain/post friction as well as perturbation of the surrounding electric and hydrodynamic fields are neglected: the post is thus reduced to a virtual uncrossable line.

Lead by the above example, we may then use, in our model, an equivalent hydrodynamic picture of the problem: a neutral coil colliding with a post in a solvent flowing at speed μE. Collective effects are thus expected, as opposed to the Rouse picture where the collision is controlled by mere local forces along the backbone.

2.1 Trapping thresholds

When the drifting coil hits the post, the chain deforms (and is likely to be trapped) if the resistance force F, exerted by the post, is greater than k_BT/R_g. From the discussion in 1.2, we expect trapping above a field $E_{cHI} \sim (k_BT/\mu\eta a^2)N^{-2\nu}$, whereas a local force picture would give $E_{cR} \sim (k_BT/qa)N^{-(1+\nu)}$. For $E < E_c$, the coil slides along the post, and its effective mobility is mostly not affected.

The trapping thresholds can be understood in terms of relaxation times. The above condition over F also reads $\xi V > k_BT/R_g$, where $V = \mu E$ is the free drift velocity, and ξ is the model dependent friction. Let τ be the chain's relaxation time, *i.e.* the time a coil takes to diffuse over its own size. From Einstein's relation we have $R_g^2/\tau \sim k_BT/\xi$, which leads to $V > R_g/\tau$ for the trapping condition. In other words, the polymer will hook onto the post if the post penetrates in the coil faster than the chain can reorganize to avoid it. Note that τ is the Rouse relaxation

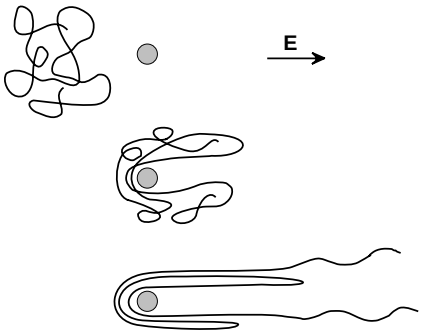

Fig. 2. Schematic picture of a polyelectrolyte/post collision during electrophoretic drag.

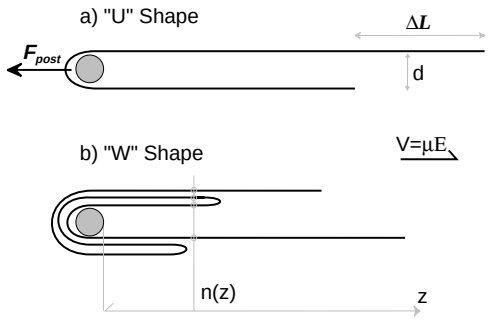

Fig. 3. Schematic typical extended chain configurations under strong field (or under strong solvent flow).

time in the local friction model, and the Zimm time when hydrodynamic interactions are taken into account.

2.2 Unhooking

For $E > E_c$ there is an effective polymer/post interaction. The coil, seen as a 3D random walk, is crushed against the post, and loops of polymer are pulled on each side (Fig. 2). Loops elongate, and a pulley-like competition takes place: the longer loops phagocyte the shorter ones until release, when all monomers have been pulled onto one side. Since tension vanishes at its downstream end, each loop is equivalent to a couple of adjacent strands (half loops): a polyelectrolyte trapped on a post can thus be roughly pictured as a dynamic collection of connected strands stretched by neutral and electric forces, similarly to the description of a single strand in 1.2.

The broad initial loop lengths distribution smoothes the field regime limits, all the more so as elongation is coupled to competition, nonetheless one can distinguish "intermediate" and "strong" field regimes.

Intermediate field regime: the average half loop conformation is a trumpet. Extensions do not scale like contour lengths, therefore, as seen in the first section, the whole set of pulling forces, that drive the elongation and unhooking dynamics, obeys different scaling laws whether hydrodynamic interactions are ignored or not.

It is difficult to go beyond this rough qualitative difference between the models. However, Sevick and Williams have shown, in the Rouse picture, that a large part of the average unhooking time is spent in a final hairpin configuration (Fig. 3a) [7]. Let us thus focus on this simpler ultimate stage, which can moreover be seen as the elementary competition process between two given loops at any step of the unhooking.

Consider a U-shape configuration in the trumpet regime: $\mathcal{L}_{i=1,2}$ are the extensions of the two strands ($\mathcal{L}_1 > \mathcal{L}_2$), $N_i a$ their contour lengths, and $v = a\, d\mathcal{L}_1/dt$ the elongation exchange rate. The trumpets are pulled by electric forces F_i, with $F_{iHI} = \eta \mathcal{L}_i \mu E$, and $F_{iR} = N_i q E$: initial extensions and unhooking dynamics both scale differently according to the model. Time evolution is determined by the balance of the combined electro-hydrodynamic forces on the strands: $F_1 - \eta\mathcal{L}_1 v = F_2 + \eta\mathcal{L}_2 v$ ($\equiv 1/2 F_{post}$), $\mathcal{L}_i$ depending itself on F_{post}. In a very rough picture where $v \sim \mu E$ and with a release time T_f estimated by $v \sim \mathcal{L}_{2,t=0}/T_f$ one derives, in good solvent ($\nu = 3/5$): $T_{fHI} \sim E\, N^3$, whereas $T_{fR} \sim E^{-1/3} N^{5/3}$.

In conclusion, since they change the pulling forces, hydrodynamic interactions strongly affect the release time, even here, starting from a rather stretched configuration. Preliminary steps being more "compact" (bigger difference between $\mathcal{L}$ and Na), one expects this effect to be all the more important.

Strong field regime: when the drag force $\eta\mu\, Na\, E$ (or equivalently NqE in the electric language) is larger than $k_B T/a$, in either model, all larger loops are fully extended, extensions and contour lengths scale alike. At this level of description, the Rouse-like model and our hydrodynamic picture become equivalent. In addition, one should emphasize that, DNA being quite rigid a polymer, practical electrophoresis conditions may often take place in this regime.

However, from the equivalent hydrodynamic picture we see that one should also take into account interactions *between* the loops, as well as between the two strands of a given loop.

2.3 Interactions between loops

In the hydrodynamic picture, under intermediate or strong field, the polymer is stretched into a set of loops (respectively trumpets or stems) dragged by the solvent flow. Let us analyze how these objects hydrodynamically interact.

Consider the simplest situation, in the strong field regime: a polymer trapped in a balanced U-shape configuration of elongation $\mathcal{L}$ (Fig. 3a, with $\Delta\mathcal{L} = 0$). The two adjacent strands are separated by a distance d, with $d \ll \mathcal{L}$: their global friction is equivalent to the friction of one strand alone, so the post exerts on the whole polymer a force $F_{post} \sim \eta\mathcal{L}\mu E$. The effective tension on each strand is thus half the tension a single strand would be submitted to, in the absence of such an interaction. Obviously, this mutual screening is all the more relevant in earlier, more entangled, steps of the unhooking, when a large number of loops "share" the overall friction. Due to these inter loop interactions, the forces acting on each loop are reduced, by a factor that depends on the instantaneous number of

loops. In both regimes we may thus expect an effect on the unhooking dynamics. Moreover, in the intermediate regime, the elongation of the trumpets depend on these respective tensions, and are thus reduced as well, so the global friction, that determines the tensions in feedback, is also affected.

To illustrate this, let us go back to the stretched U-shape configuration (Fig. 3a): a screened drag force acts on the adjacent portions, whereas the extra length $\Delta\mathcal{L}$ of the longer strand keeps its original friction. Since only this excess length $\Delta\mathcal{L}$ drives the unhooking, the release time in this particular configuration happens to be unaffected by the inter loop interaction. Yet, one can check that in the "W" configuration (Fig. 3b), the unhooking is indeed slowed down roughly by a factor 2, until a U-type configuration is reached.

Lead by this observation, we wish to determine if the hydrodynamic interactions between the polymer loops qualitatively modify the general unhooking process. These interactions appear both in the intermediate and in the strong field regimes but, as they are not necessary in the first case to discriminate between the models, we will focus now on the strong field regime. Due to the intricacy of this process only a simplified numerical simulation was attempted.

3 Simulations: inter-loop interactions in strong fields

3.1 Model

A polymer/post collision is roughly composed of three overlapping steps: impact, loop stretching, and competition. With the strong field assumption we simplify this scenario. In this regime, deformation around the post and elongation are much faster than chain diffusion, therefore we may neglect internal reorganizations of the coil at impact: the initial set of loops is obtained by simply splitting the 3D random walk with a plane (trajectory of the post in the coil). The direction along the post being irrelevant, the preliminary impact step reduces thus to generating 1D random walks, and splitting them at a distance b (impact parameter) from their center of mass.

After impact the loops elongate and, because of their broad distribution of lengths, competition takes place simultaneously: the shortest loops are absorbed before the longer ones reach full extension. Putting this aspect aside, we have chosen an artificial but manageable starting point: *all* initial loops fully stretch, and the competition starts in this configuration. The unhooking process is also simplified, being reduced to pulley-like competitions for strands under strong tension (and thus at full extension), and free drift for loops flipped over the post, until they reach extension again. Apart from this toppling over the post, the present unhooking process differs from the usual hernia competition discussed in [15,16], by the addition of collective effects (hydrodynamic screening), and by the broad initial length distribution. The process should thus be immediately sensitive to the walks' initial realization and finite size. The minimal dynamics allows us to probe a wide range of chain sizes, and to average over large samples. However, the neglected loop stretching step after impact could also contribute to the total collision time, and certainly controls part of the sensitivity to the impact parameter. Nonetheless, the consistency of our results with those of more elaborate simulations [7,8] indicates *a posteriori* that this numerical model contains most of the relevant physical information.

In a realistic description, the interactions should include shear flows due to the loops' relative motions, as well as "core" effects, friction being higher for the outer loops than for those nested inside; and finally, due to its finite radius, one should distinguish the inter-loop interactions within one side and between the two sides of the post. We proceed to a much simplified computation of the interactions.

The chain is globally pulled by the solvent, flowing at speed μE. At each step, all connected couples of loops evolve according to a pulley-like competition determined by their relative frictions. Let then $n(z)$ be the number of strands under tension at a downstream distance z from the obstacle (Fig. 3b). The effective drag flow "seen" by a loop segment at a distance z is approximated by $\mu E/n(z)$, in a mean field like picture; thus the total force applied on a strand of length $\mathcal{L}$, *in a given configuration* of the chain, is $\eta\mu E\int_0^{\mathcal{L}} 1/n(z)dz$ (the total force on the chain, $\eta\mu E\mathcal{L}_{chain}$, being conserved).

3.2 Results and comparison with previous data

We focus here on the parameters that eventually take part in the size separation performances of the collision and in the post spacing optimization: the release time T_f (elapsed between the beginning of the loop competition and the moment of untrapping), and the chain's downstream extension at release (through the position of its center of mass Zc).

As shown in Figure 4, the average release time scales like the molecular weight N, both in the Rouse-like and in the hydrodynamic models. This result is similar to those obtained by previous simulations [7]. In the first model, this scaling can be expected: the time evolution equations are homothetic [15,16], and the loop length initial distribution obeys a power law (apart for the unit length cut-off determined by the persistence length). Consequently, the initial cut-off dependent steps having a negligible contribution, the total release time is proportional to N. However, this can no longer be readily predicted in the complete hydrodynamic model, as T_f is partly controlled by the *number* of loops, which has a non-extensive behavior, initially scaling like $N^{1/2}$.

As shown in Figure 5, the unhooking time follows a self-similar distribution regarding system size, that is conserved and roughly unchanged whether hydrodynamic interactions are taken into account or not. This kind of self-similarity was also found in models describing hernia competition under electrophoresis [15,16].

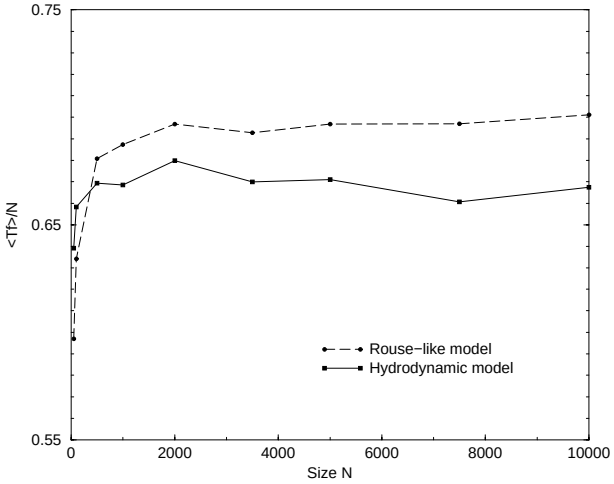

Fig. 4. The collision time is averaged for 5000 walks, with $b = 0$. Both the persistence length a, and the free drift velocity μE are set to unity. Finite size effects appear for $N < 100$.

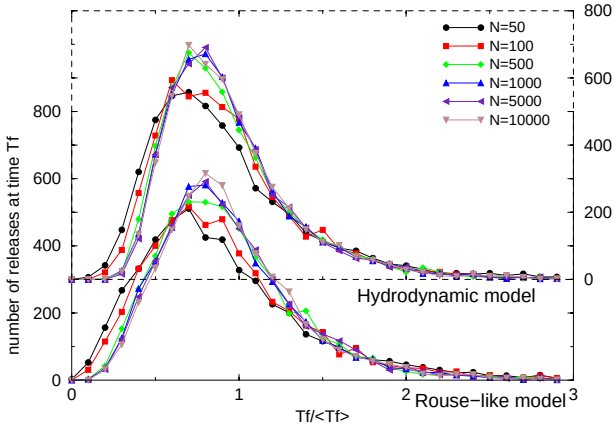

Fig. 5. Distribution of release time for a sample of 5000 centered polymers ($b = 0$). The plots are rescaled with the average release time for each size: they stabilize for $N > 100$. The distribution tails are exponential.

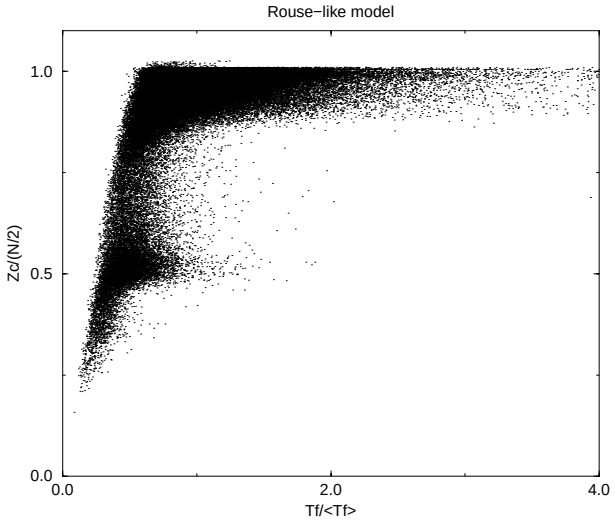

Fig. 6. The chains' final extension is plotted against the corresponding release time, in reduced values, for a sample of 10^5 chains of length $N = 200$, in the case of *centered* collisions ($b = 0$). This extension is estimated with Zc, the final downstream distance of the chain's center of mass to the post. As in [7], Zc is roughly linear for $(T_f/\langle T_f\rangle) \leq 0.5$, the saturation at $Zc = N/2$ showing the importance of balance hairpin configurations. One also sees the trace of double hairpins at $Zc = N/4$.

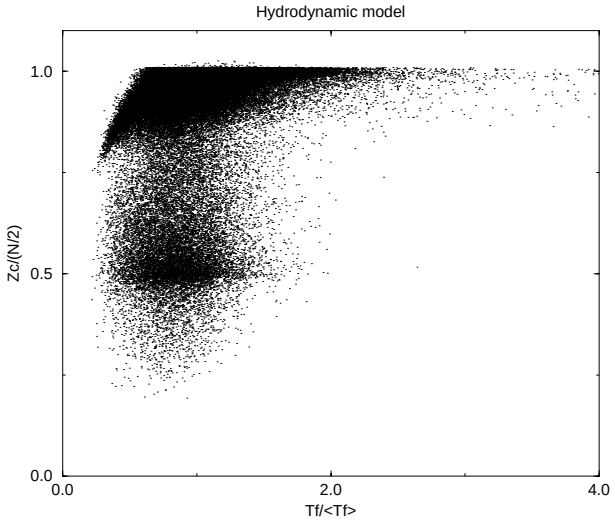

Fig. 7. We take in account inter-loops interactions using the same sample as in Figure 6.

Finally, comparing the data shown in Figures 6 and 7, one observes that the hydrodynamic model roughly gives the same final elongation distribution as in the Rouse-like one. Figure 6 is, in addition, in fairly good quantitative agreement with the data presented by Sevick and Williams, and, like these authors, we notice the dominant statistical weight of final hairpin configurations (as discussed in Sect. 2.2). We also obtain, in both models, an exponential decrease of T_f with the impact parameter b (data not shown), in consistency with [7] (however, due to our assumption for the initial stretching steps, we do not expect our model to be really adequate for describing very off-centered impacts).

In conclusion, in strong field regime and given our simplified numerical model, hydrodynamic screening between chain loops does not noticeably affect the average geometrical and time characteristics of the unhooking process: the scaling and statistical features of the release time, as well as the chains' extensions at release, keep the properties given in the Rouse-like approach.

Focusing on details, we refine the comparison between the Rouse-like and the hydrodynamic models. It appears from Figure 4 that, surprisingly, the mean unhooking time is *shorter* in the hydrodynamic model, whereas one could expect the hydrodynamic screening to slow down the untrapping, as it globally reduces the dragging forces. Figure 8 indicates a slower evolution at the beginning of the unhooking in the hydrodynamic case. Finally, comparing Figure 6 with Figure 7 suggests that including interactions

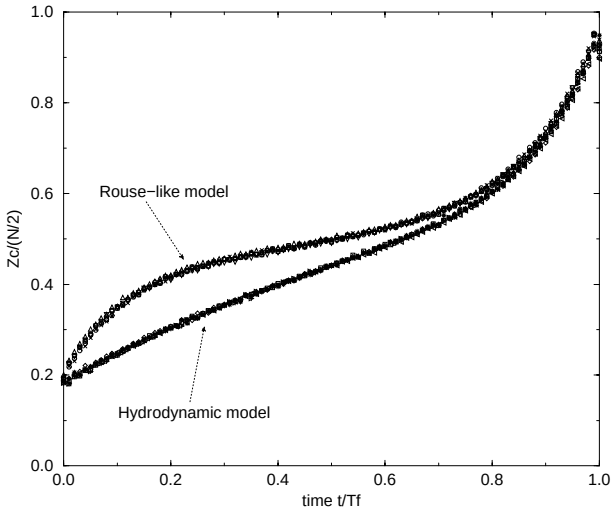

Fig. 8. Zc is the downstream distance of the chains' center of mass to the post. Its time evolution is rescaled with the actual final release time T_f for *each* chain, then average over a large sample of chains. Plots for several chain sizes (N ranging from 50 to 5000) collapse on one curve in each model. Impacts are centered ($b = 0$).

results in longer trapping times when the releases occur in many loops configurations (typically $Zc(T_f) \leq N/4$), whereas very stretched configurations releases ($Zc \sim N/2$) are shifted to shorter times. This point can also be seen in the slightly sharper distributions in the hydrodynamic model shown in Figure 5. A possible explanation consistent with all these observations is that the screening is very non-uniform along the chain: in the initial distribution of loops there is a large number of rather small loops ($\mathcal{L} \ll N^{1/2}$), and a few very long loops ($\mathcal{L} \sim N$) (usual properties of random walks [17]); in our hydrodynamic model, the friction sharing implies that the short loops are under very reduced tension, and are thus "frozen". One can then speculate that, because of these interactions, the longest loops, which drive the unhooking, emerge immediately and more efficiently than in the more "egalitarian" local force model. As a final remark, although release times and extensions are very similar in both models, the dynamical differences at short times (Fig. 8) may be important under pulsed field conditions.

4 Discussion

In this paper, using the ideas developed in [9,10], we have given a theoretical analysis of the interaction between a polyelectrolyte and a fixed post under electrophoretic conditions. Our approach yields a new interaction threshold, and predicts strong qualitative modifications to the previous descriptions in moderate field regimes. Under strong electric field however, our simulations show that the remaining inter-loop interactions do not affect the global pictures emerging from the analysis using simplified Rouse-like models presented in [7,8]; they validate thus the previous conclusions concerning polyelectrolyte fractionation by single collision processes. Let us note that the hydrodynamic interactions produce nonetheless dynamical effects that may show up in transient or pulsed fields.

We have developed a simple numerical model for the strong field regime which leads, in its Rouse-like version, to results quantitatively similar to those obtained in more complex numerical approaches (Langevin and Brownian dynamics [7,8]). This agreement allows us to test much larger chains than in these simulations, and suggests that neither a precise description of the chain's elasticity nor molecular dynamics seem relevant. The model could be improved however to better describe the initial stretching step and thus the off-centered impacts.

In conclusion, let us note the different aspects that could be also included for a more realistic description. In particular, the post is modeled here as a virtual obstacle, whereas in a more realistic picture, its actual size, geometry and surface properties, result in electro-osmotic and hydrodynamic flows. We have also assumed the absence of boundary effects, although migrations often take place in slabs where the walls screen the hydrodynamic interactions, generating nonetheless important osmotic flows [4,18]. Furthermore, under strong fields, several complications may arise: the actual mobility of DNA depends slightly on the orientation of its segments [19], and is thus expected to change as the chain reaches strong extensions; also, non linear couplings between mechanical forces and electric drag can modify somewhat the analysis.

References

1. B.M. Olivera, P. Baine, N. Davidson, Biopolymers **2**, 245 (1974).
2. L.S. Lerman, H.L. Frisch, Biopolymers **21**, 995 (1982).
3. A.T. Andrews, *Electrophoresis: Theory, Techniques and Biochemical and Clinical Applications* (Clarendon, Oxford, 1986), 2nd edn.
4. W.D. Volkmuth, R.H. Austin, Nature **358**, 600 (1992).
5. R.H. Austin, W.D. Volkmuth, Analusis **21**, 235 (1993).
6. W.D. Volkmuth, T.A.J. Duke, M.C. Wu, R.H. Austin, A. Szabo, Phys. Rev. Lett. **72**, 2117 (1994).
7. E.M. Sevick, D.R.M. Williams, Phys. Rev. Lett. **76**, 2595 (1996).
8. G.I. Nixon, G.W. Slater, Phys. Rev. E **50**, 5033 (1994).
9. D. Long, J.L. Viovy, A. Ajdari, Phys. Rev. Lett. **76**, 3858 (1996).
10. D. Long, J.L. Viovy, A. Ajdari, J. Phys.: Condens. Matter **8**, 9471 (1996).
11. G.S. Manning, J. Phys. Chem., **85** 1506 (1981).
12. J.L. Barrat, J.F. Joanny, Adv. Chem. Phys. **94**, 1 (1996).
13. F. Brochard-Wyart, H. Hervet, P. Pincus, Europhys. Lett. **26**, 511 (1994).
14. F. Brochard-Wyart, Europhys. Lett. **30**, 387 (1995).
15. D. Long, J.L. Viovy, Physica A **244**, 238 (1997).
16. J.M. Deutsch, Phys. Rev. Lett., **59**, 1255 (1987).
17. W. Feller, *An Introduction to Probability Theory and Its Applications* (John Wiley and Sons, 1968).
18. O.B. Bakajin, T.A.J. Duke, C.F. Chou, S.S. Chan, R.H. Austin, E.C. Cox, Phys. Rev. Lett. **80**, 2737 (1998).
19. D. Stigter, J. Chem. Phys. **82**, 1424 (1978).